Cell, Vol. 107, 789–800, December 14, 2001, Copyright ©2001 by Cell Press

# The Membrane-Anchored MMP Inhibitor RECK Is a Key Regulator of Extracellular Matrix Integrity and Angiogenesis

Junseo Oh,[1] Rei Takahashi,[2] Shunya Kondo,[1] Akira Mizoguchi,[3] Eijiro Adachi,[5] Regina M. Sasahara,[1,10] Sachiko Nishimura,[1,6] Yukio Imamura,[1] Hitoshi Kitayama,[1] David B. Alexander,[1] Chizuka Ide,[3] Thomas P. Horan,[7] Tsutomu Arakawa,[7,11] Hisahito Yoshida,[4] Shin-ichi Nishikawa,[4] Yoshifumi Itoh,[8] Motoharu Seiki,[8] Shigeyoshi Itohara,[6] Chiaki Takahashi,[1,12] and Makoto Noda[1,9]

[1] Department of Molecular Oncology
[2] Department of Pathology and Tumor Biology
[3] Department of Anatomy and Neurobiology
[4] Department of Molecular Genetics
Kyoto University Graduate School of Medicine
Yoshida-Konoe-cho, Sakyo-ku
Kyoto 606-8501
Japan
[5] Department of Molecular Morphology
Kitasato University Graduate School of Medical Sciences
Sagamihara
Kanagawa 228-8555
Japan
[6] RIKEN Brain Research Institute
Wako-shi
Saitama 351-0198
Japan
[7] Amgen Inc.
Amgen Center
Thousand Oaks, California 91320
[8] Department of Cancer Research
Institute of Medical Science
University of Tokyo
Tokyo 108-0071
Japan

## Summary

**Matrix metalloproteinases (MMPs) are essential for proper extracellular matrix remodeling. We previously found that a membrane-anchored glycoprotein, RECK, negatively regulates MMP-9 and inhibits tumor invasion and metastasis. Here we show that RECK regulates two other MMPs, MMP-2 and MT1-MMP, known to be involved in cancer progression, that mice lacking a functional *RECK* gene die around E10.5 with defects in collagen fibrils, the basal lamina, and vascular development, and that this phenotype is partially suppressed by MMP-2 null mutation. Also, vascular sprouting is dramatically suppressed in tumors derived from RECK-expressing fibrosarcoma cells grown in nude mice. These results support a role for RECK in the regulation of MMP-2 in vivo and implicate RECK downregulation in tumor angiogenesis.**

[9] Correspondence: mnoda@virus.kyoto-u.ac.jp
[10] Present address: Department of Biochemistry, University of Sao Paulo, Av. Prof. Lineu Prestes 748, 05508-900, Sao Paulo, SP, Brazil
[11] Present address: Alliance Protein Laboratories, 3957 Corte Cancion, Thousand Oaks, CA 91360
[12] Present address: Adult Oncology, Dana-Farber Cancer Institute and Harvard Medical School, DN728, 44 Binney St., Boston, MA 02115

## Introduction

Extracellular matrices (ECM) consist mainly of collagen, proteoglycans, and glycoproteins such as laminin and fibronectin. The ECM provides an essential framework upon which cells grow, migrate, and differentiate, and it is essential that the ECM undergo continuous remodeling during animal growth and development (Vu and Werb, 2000). A family of extracellular proteases called matrix metalloproteinases (MMPs) are essential for proper ECM remodeling (reviewed in Birkedal-Hansen, 1995; Vu and Werb, 2000). MMPs are produced as inactive precursors whose $NH_2$-terminal portion has to be removed to manifest the active enzyme (Nagase and Woessner, 1999). Also, a family of MMP inhibitor proteins known as tissue inhibitors of metalloproteinases (TIMPs) are able to inhibit MMP activity in vitro (Brew et al., 2000). Thus, MMP activity is potentially regulated at three steps: (1) gene expression, (2) proenzyme processing, and (3) inhibition of enzymatic activity (Hidalgo and Eckhardt, 2001).

In early development, blood vessel formation occurs by a process termed vasculogenesis, in which endothelial cells proliferate, differentiate, and coalesce to form a primitive tubular network referred to as the vascular plexus. This initial network is modified through pruning and vessel enlargement to form the interconnecting branching patterns characteristic of the mature vasculature, a process termed angiogenic remodeling (Yancopoulos et al., 2000). During this process, vessel walls also mature, as endothelial cells integrate tightly with mural cells (such as smooth muscle cells and pericytes) and the surrounding ECM. A different process termed angiogenic sprouting, which involves sprouting from existing vessels into a previously avascular tissue, is responsible for vascularization of certain tissues during normal development, such as the neural tube, and for most new vessel formation in the adult (Folkman and D'Amore, 1996; Risau, 1997; Hanahan, 1997; Yancopoulos et al., 2000). MMPs are known to play an important role during each of these steps (Stetler-Stevenson, 1999).

ECM remodeling is also important in certain pathological conditions, such as wound healing, osteoporosis, rheumatoid arthritis, and cancer (Werb, 1997). Cancer cells feed themselves by recruiting blood vessels into the tumor mass (tumor angiogenesis) and escape from their original sites by penetrating the basal lamina and other ECM structures (invasion and metastasis) (Hanahan and Folkman, 1996; Stetler-Stevenson, 1999). MMP-2, MMP-9, and MT1-MMP are all potentially involved in carcinogenesis, since correlation between

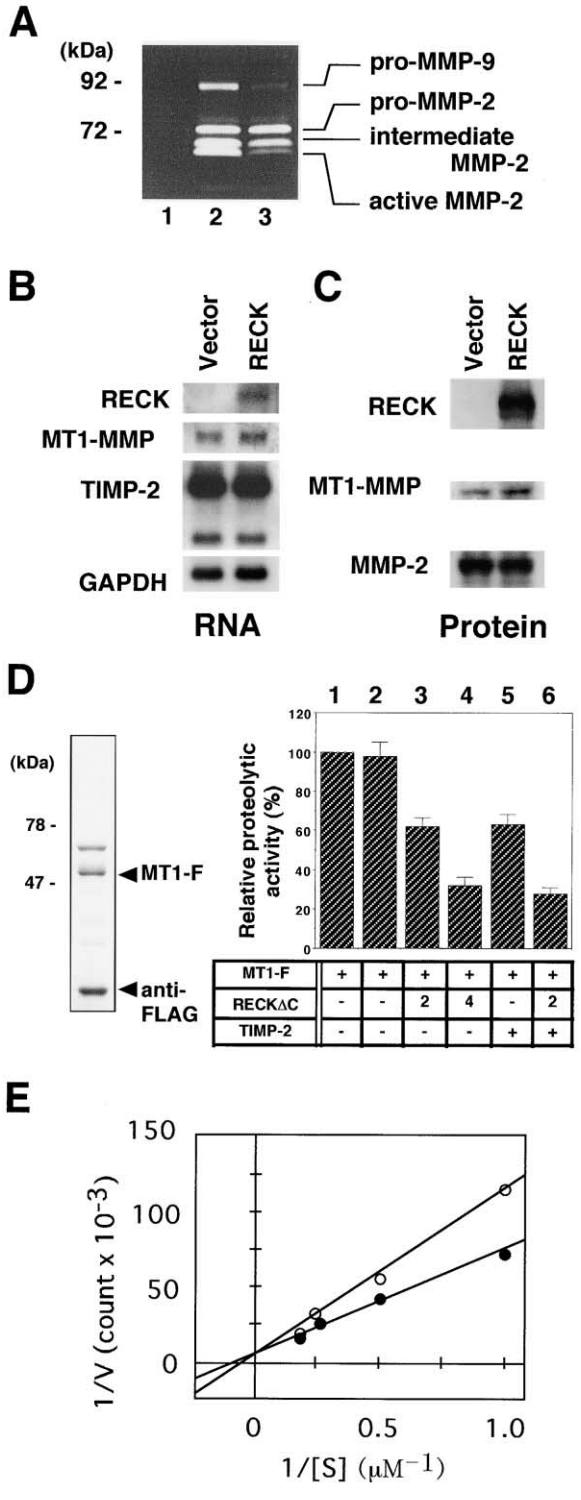


Figure 1. RECK Regulates Three MMPs

(A) Effects of *RECK* on the production of gelatinolytic enzymes by HT1080 cells. Either fresh medium (lane 1), conditioned medium prepared from a pool of vector-transfected HT1080 cells (lane 2), or conditioned media from *RECK*-transfected HT1080 cells (lane 3) was analyzed by gelatin zymography. The molecular species corresponding to each band is indicated on the right.

(B and C) Effects of *RECK* on the expression of MT1-MMP, MMP-2, and TIMP-2 in HT1080 cells. The mRNA (B) or total proteins (C) extracted from HT1080 transfectants were analyzed by RNA blot hybridization or immunoblot assay, respectively.

(D) Effects of RECK on MT1-MMP activity in vitro. Left panel: MT1-F protein expressed in *E. coli* and partially purified was analyzed by SDS-PAGE (stained with Coomassie blue). The identity of the top band is unknown. Right panel: the bead-bound MT1-F was mixed with 4 pmol BSA (bar 2), 2 pmol (bars 3, 6), or 4 pmol (bar 4) hRECKΔC in the absence (bars 1–4) or presence (bars 5 and 6) of 0.25 pmol TIMP-2, and proteolytic activity was measured using a fluorescent MMP substrate. Error bars represent SE from three independent measurements.

(E) Effects of RECK on APMA-activated MMP-2. Pro-MMP-2 was activated with APMA and its proteolytic activity measured using increasing concentrations (1–10 μM) of fluorescent MMP substrate in the absence (filled circle) or presence (open circle) of hRECKΔC (3.5 pmol). Data are presented as a double reciprocal Lineweaver-Burk plot. The $K_i$ value obtained from these data is 80 nM.

their activity and the malignancy of tumors has been documented in a number of studies (Davies et al., 1993; Yamamoto et al., 1996; Kahari and Saarialho-Kere, 1999; Coussens et al., 2000). Moreover, in preclinical studies, synthetic MMP inhibitors have been found to inhibit tumor growth and metastasis (Hidalgo and Eckhardt, 2001).

The *RECK* gene was isolated by an expression cloning strategy designed to isolate human cDNAs inducing flat reversion in a *v*-Ki-*ras*-transformed NIH3T3 cell line (Noda et al., 1989; Kitayama et al., 1989; Takahashi et al., 1996). The *RECK*-encoded glycoprotein (molecular weight 110,000) contains serine protease inhibitor-like domains and is associated with the cell membrane through a carboxy-terminal glycosylphosphatidylinositol (GPI)-modification (Takahashi et al., 1998). While the *RECK* gene is widely expressed in various human organs, its expression is low or undetectable in many tumor-derived cell lines; also, *RECK* expression can be downregulated by several oncogenes, including *ras* (Takahashi et al., 1998; Sasahara et al., 1999). When *RECK* gene expression was artificially restored in several tumor-derived cell lines, the amount of extracellular pro-MMP-9 produced by these cells was reduced, and their invasive and metastatic potentials were suppressed (Takahashi et al., 1998), suggesting a role for RECK in the regulation of MMP-9 and tumor malignancy.

In the present study, we further evaluated the biochemical activities of RECK and explored its biological functions in vivo through gene targeting experiments as well as tumor transplantation experiments in mice. The results indicate that RECK negatively regulates two other MMPs, MMP-2 and MT1-MMP, and document the importance of RECK in the regulation of ECM remodeling and blood vessel formation.

## Results

### Downregulation of Active MMP-2 by *RECK*

Since RECK was originally identified as a membrane-associated negative regulator of MMP-9 (Takahashi et al., 1998), we used the human fibrosarcoma-derived cell line HT1080, which expresses both MMP-2 and MMP-9 but does not express RECK, to determine if RECK might also regulate MMP-2. When conditioned medium from HT1080 cells transfected with a control vector was ana-

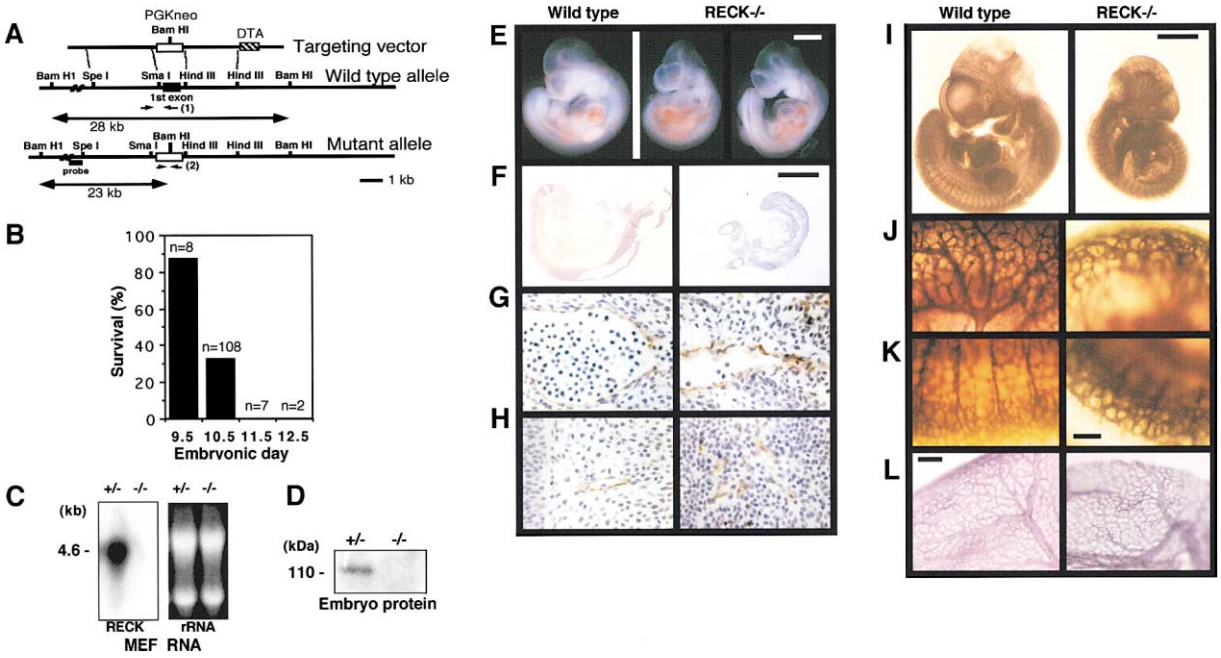


Figure 2. Generation of *RECK*-Deficient Mice

(A) Targeting strategy.

(B) Proportion of surviving *RECK*$^{-/-}$ embryos at indicated stages. n, number of embryos observed.

(C) RNA blot analysis for *RECK* expression in cells from heterozygous (+/−) or homozygous (−/−) mutant embryos (left panel). An ethidium-stained membrane is also shown (right panel).

(D) Immunoblot analysis for RECK protein in whole embryo lysates.

(E–L) Morphology of the wild-type (left panels) and *RECK*$^{-/-}$ (right panels) E10.5 embryos.

(E) Unfixed embryos.

(F) Whole embryo sections stained with anti-RECK antibodies.

(G and H) Disarray of vascular endothelial cells in the *RECK*$^{-/-}$ embryo. Relatively large (G) and small (H) blood vessels in sections stained with anti-CD31 antibodies are shown.

(I–K) Visualization of the vascular network in the embryo proper by whole-mount immunohistochemistry. (I) Embryos stained with anti-CD31 antibodies. Higher magnification of the head regions (J) and the trunk regions (K) are also shown.

(L) Vascular network in yolk sacs stained with anti-Flk-1 antibodies.

Scale bar: 0.5 mm in E and J; 1 mm in F; 50 μm in G–I; 0.2 mm in K–M.

lyzed by gelatin zymography, we could detect four major bands: the 92 kilodalton (kDa) band corresponding to the molecular weight (MW) of pro-MMP-9, and a triplet of bands around 70 kDa corresponding (from top to bottom) to the MW of the pro-, intermediate, and active forms of MMP-2 (Figure 1A, lane 2). When *RECK* was expressed in these cells, the amount of secreted pro-MMP-9 and active MMP-2 were significantly reduced (Figure 1A, lane 3). A less drastic, but reproducible, reduction in the amount of the intermediate form of MMP-2 was also noted. Immunoblot assays, however, indicated that *RECK* did not affect the total amount of MMP-2 protein associated with the cells (Figure 1C). Interestingly, we previously showed that the amount of MMP-9 mRNA expressed by HT1080 cells is not affected by *RECK* expression (Takahashi et al., 1998). Thus, RECK regulates MMP-2 and MMP-9 posttranscriptionally.

### Inhibition of MT1-MMP by RECK

Processing of pro-MMP-2 takes place by two consecutive proteolytic cleavages which occur preferentially at the plasma membrane (reviewed in Ellerbroek and Stack, 1999). First, a membrane-anchored ternary complex consisting of MT1-MMP, TIMP-2, and pro-MMP-2 is formed on the cell surface, and the pro-MMP-2 is cleaved at a specific site ($Asn^{37}$-$Leu^{38}$ in the human protein) by a second MT1-MMP molecule to yield the intermediate form of MMP-2. Second, the removal of the residual prodomain is achieved through intermolecular, autoproteolytic cleavage, and is accompanied by release of active MMP-2 from the membrane. Thus, a simple mechanism which would explain the observed downregulation of active MMP-2 would be the upregulation of TIMP-2, since TIMP-2 is known to inhibit MT1-MMP as well as active MMP-2 in vitro. *RECK* does not, however, alter the level of TIMP-2 mRNA (Figure 1B). Downregulation of MT1-MMP expression could also explain our finding; however, the level of MT1-MMP expression was not reduced by *RECK* (Figures 1B and 1C). We therefore tested the possibility of direct enzymatic inhibition of MT1-MMP activity using purified recombinant proteins. In this assay, we employed a soluble MT1-MMP protein (MT1-F; Kinoshita et al., 1998) lacking the $NH_2$-terminal prodomain and containing the FLAG-epitope in place of the COOH-terminal transmembrane domain (Figure 1D, left panel). The RECK protein employed in this assay (hRECKΔC) was also a soluble form which lacks the COOH-terminal GPI-anchoring domain but re-

tains invasion-suppressing activity (Takahashi et al., 1998). Consistent with previous observations, the activity of MT1-F, as assayed using a fluorescent MMP substrate (Mca-P-L-G-L-Dpa-A-R; Knight et al., 1992), was sensitive to TIMP-2 (Figure 1D, right panel, bar 5). In this assay, the hRECKΔC protein inhibited MT1-F activity in a dose-dependent manner (Figure 1D, bars 3 and 4), and the effects of hRECKΔC and TIMP-2 were additive (Figure 1D, bar 6). These results suggest that RECK can directly inhibit MT1-MMP.

### Inhibition of MMP-2 by RECK

The data in Figure 1A suggest that the second step of pro-MMP-2 processing (i.e. conversion of the intermediate form to the active form by autoproteolysis) is dramatically inhibited by *RECK* expression. We therefore examined the effects of purified RECK protein (hRECKΔC) on the activity of MMP-2 in vitro. Purified recombinant pro-MMP-2 was activated by treatment with a sulfhydryl-reactive compound, aminophenylmercuric acetate (APMA), and the resulting proteolytic activity against Mca-P-L-G-L-Dpa-A-R was measured in the absence or presence of hRECKΔC. A Lineweaver-Burk plot of the data shows that hRECKΔC competitively inhibits MMP-2 with a calculated Ki value of 80 nM (Figure 1E), which is similar to the Ki value for this protein against MMP-9 (Takahashi et al., 1998). The results from these and previous experiments suggest that RECK serves as a membrane-anchored regulator for at least three MMP family members—MMP-2, MMP-9, and MT1-MMP.

### *RECK* Is Essential for Mouse Development

To understand the physiological functions of this unique MMP regulator, we generated mice lacking a functional *RECK* gene (Figure 2A). Mice heterozygous for the *RECK* mutation ($RECK^{+/-}$) were healthy and fertile, but no homozygous pups ($RECK^{-/-}$) were born. The ratio of wild-type to heterozygous offspring was about 1:2, indicating a recessive lethal phenotype. To determine the time at which the effects of *RECK* deficiency become manifest, we examined embryos from heterozygous intercrosses at different developmental stages (Figure 2B). No overt phenotype was seen in $RECK^{-/-}$ embryos at embryonic day 9.5 (E9.5) (data not shown); however, about two-thirds of the $RECK^{-/-}$ embryos died (as judged by lack of heartbeat) by E10.5, and no $RECK^{-/-}$ embryos survived beyond E11.5. The lack of *RECK* gene products in the homozygous mutant embryos was confirmed by RNA blot hybridization (Figure 2C), immunoblot assay (Figure 2D), and immunostaining of embryo sections (Figure 2F). Similar phenotypes and embryonic death of homozygous mutants were observed in mutants derived from two independent ES cells lines and in two genetic backgrounds (129/Sv and C57BL/6J).

$RECK^{-/-}$ embryos are distinct from their littermates in their smaller body sizes, a conspicuous reduction in structural integrity, and frequent abdominal hemorrhage (Figure 2E). Histological examination revealed severe disarray of mesenchymal tissues and disrupted organogenesis in the mutant embryos (Figure 2F and data not shown). In particular, vascular endothelial cells do not form tight and thin tubular structures as seen in the wild-type embryos (Figures 2G and 2H). Although vascular networks (as revealed by whole-mount immunostaining for endothelial markers) are formed in the mutant embryo as well as in the yolk sac (Figures 2I–2L, right panels), their morphology resembles primitive vascular plexuses, suggesting defects in blood vessel maturation, rather than vasculogenesis.

### Effects of *RECK* Deficiency on MMPs and ECM Proteins

Consistent with the effects of RECK on pro-MMP-2 processing in HT1080 cells described above (Figure 1A), conditioned media prepared from $RECK^{-/-}$ embryonic cells contained elevated levels of active MMP-2 compared to those from $RECK^{+/+}$ and $^{+/-}$ littermates (Figure 3A). As expected, pro-MMP-9—which is not expressed until E11 (Canete-Soler et al., 1995)—was not detected. Also, when fibroblastic cell lines (MEF) established from $RECK^{-/-}$ embryos were transfected with a *RECK*-expression vector, their conditioned media contained reduced levels of active MMP-2 (Figure 3B). Thus, the absence of *RECK* expression likely results in disinhibition of MMP-2, and presumably MT1-MMP, as predicted by the biochemical data, leading to excessive degradation of the ECM.

This hypothesis was examined by several approaches comparing $RECK^{-/-}$ and $RECK^{+/+}$ littermates. First, the MMP assay measuring proteolytic activity against Mca-P-L-G-L-Dpa-A-R indicated elevated levels of MMP activity in the conditioned medium prepared from $RECK^{-/-}$ embryonic cells (Figure 3C). Second, in situ zymography detected a much broader area exhibiting gelatinolytic activity in sections prepared from $RECK^{-/-}$ embryos (Figure 3D). Third, immunohistochemical analyses for various ECM components revealed that the amount of collagen I in the marginal zone of the neural tubes is greatly reduced in $RECK^{-/-}$ embryos (Figure 3E) and that the staining pattern for collagen IV and laminin is largely disrupted around the blood vessels and neural tubes of the mutant embryos (Figures 3F and 3G), suggesting partial destruction of the basal lamina. The staining pattern of fibronectin was also disrupted; however, the overall effect on the intensity of fibronectin staining was less pronounced (Figure 3H). Finally, electron microscopy revealed almost complete loss of collagen fibrils and an apparently discontinuous basal lamina surrounding the neural tube in the mutant embryos (compare Figure 3J with Figure 3I). Thus, the integrity of collagen fibers and the basal lamina are severely compromised in the absence of RECK. RECK, MMP-2, and MT1-MMP are all expressed in this area (Figure 3K), supporting the idea that deregulation of one or both of these MMPs is responsible for the mutant phenotype.

### Expression of RECK in Vascular Smooth Muscle Cells

In wild-type E10.5 embryos, the RECK protein is widely expressed in mesenchymal tissues and is relatively abundant in the marginal zone of the neural tube and large blood vessels such as the dorsal aorta (Figure 4A), areas of greatly impaired distribution of ECM components in $RECK^{-/-}$ embryos. Around the dorsal aorta, the staining pattern for RECK resembles that for α-smooth muscle actin (SMA), suggesting that RECK expression

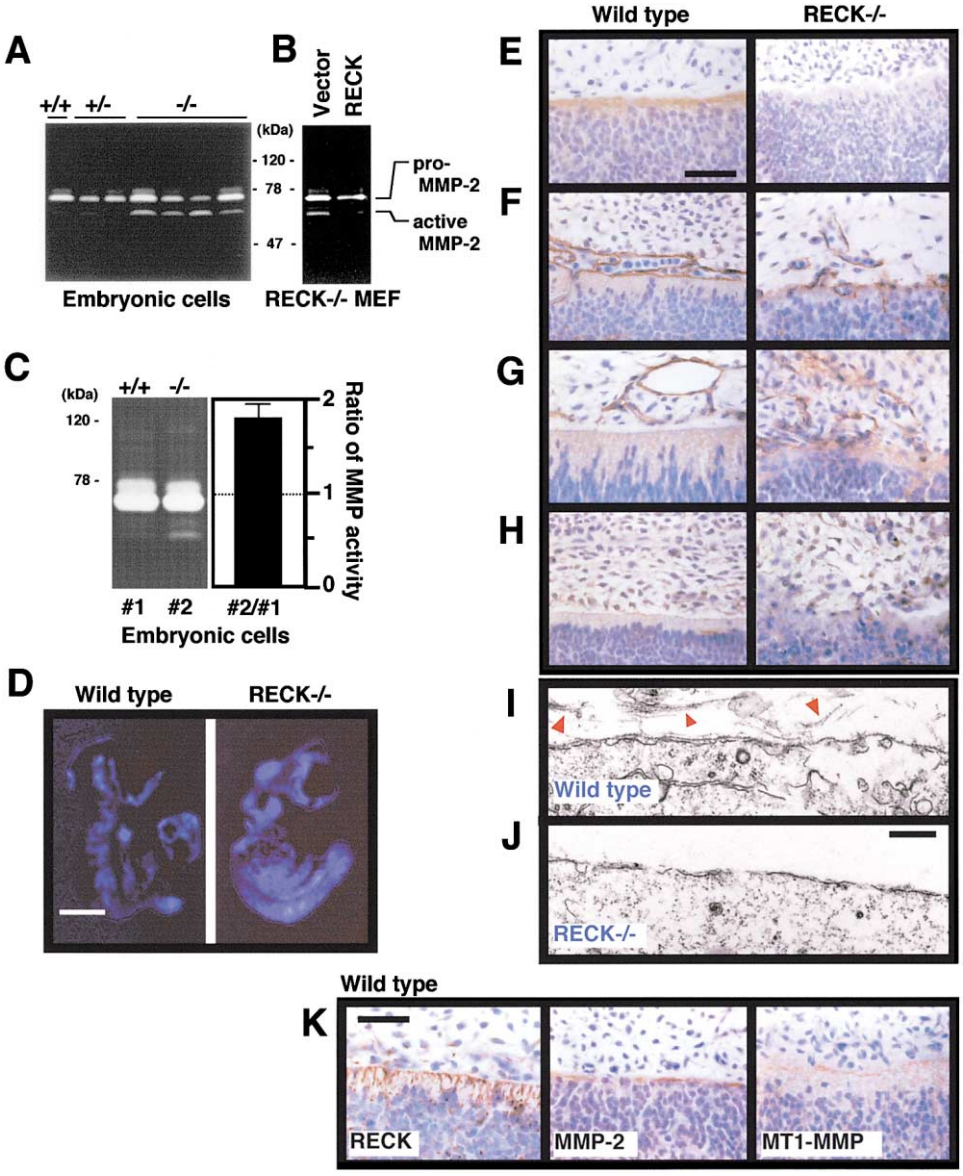


Figure 3. Effects of *RECK* Mutation on MMP-2 Processing and ECM Proteins In Vivo

(A) Increased pro-MMP-2 processing in *RECK*$^{-/-}$ cells. Conditioned media from cultured whole embryonic cells were subjected to gelatin zymography. The genotype of each embryo is shown above.

(B) Suppression of MMP-2 processing by RECK. Conditioned media from *RECK*$^{-/-}$ MEF transfected with the control vector or the vector containing *hRECK* cDNA were analyzed by gelatin zymography.

(C) Increased MMP activity in *RECK*$^{-/-}$ cells. Conditioned media from cultured embryonic cells (prepared from a pairs of littermates: #1, #2) were subjected to gelatin zymography (left panel) and their proteolytic activity against a fluorescent MMP substrate measured (right panel). The genotype of each embryo is shown above (left panel). MMP activities were compared between a pair of littermates (#1 versus #2) and presented as a ratio (right panel). Error bar represents SE from three independent measurements. Similar results were obtained with three pairs of littermates.

(D) In situ zymography of E10.25 embryos. Serial, parasagittal sections of three wild-type and three *RECK*$^{-/-}$ embryos at E10.25 (alive) were prepared and subjected to in situ zymography. A typical result from each group is shown. Essentially no gelatinolytic activity was detected with the control film containing an MMP inhibitor, 1,10-phenanthroline (not shown).

(E–H) Effects of the RECK mutation on ECM proteins. The borders between neuroepithelium and mesenchyme in the wild-type (left) or the *RECK*$^{-/-}$ (right) E10.5 embryo stained with antibodies against collagen I (E), collagen IV (F), laminin (G), or fibronectin (H) are shown.

(I and J) Ultrastructure of the outer surface of the neural tube in a wild-type (I) or a *RECK*$^{-/-}$ E10.5 embryo (J). Collagen fibrils (arrowhead) were rarely found in *RECK*$^{-/-}$ embryos.

Scale bar: 1 mm in D; 50 μm in E–H and K; 0.5 μm in I and J.

(K) The border between the marginal zone of the neural tube and the adjacent mesenchymal tissue in the wild-type E10.5 embryo stained with antibodies against RECK (left), MMP-2 (middle), and MT1-MMP (right).

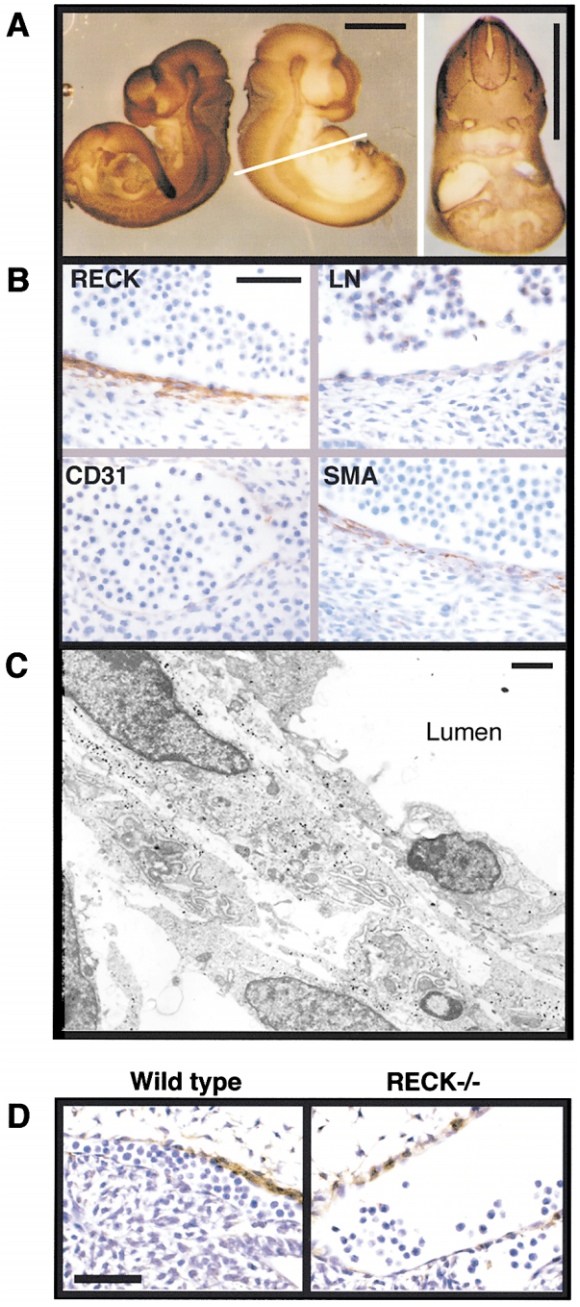


Figure 4. Tissue Distribution of RECK and Other Proteins in E10.5 Embryos

(A) A wild-type embryo was cut sagittally into two pieces, and whole-mount immunostaining was performed with (left) or without (middle) anti-RECK antibodies. The anterior half of the embryo cut transversally at the abdominal level (as shown in the middle figure) was also stained with anti-RECK antibodies (right).

(B) Large blood vessels (dorsal aorta) in the wild-type embryo stained with antibodies against RECK, laminin (LN), CD31, or α-SMA (SMA).

(C) Immunogold electron microscopy with anti-RECK antibodies. The wall of a large blood vessel in a wild-type embryo is shown.

(D) Effects of the RECK mutation on vascular smooth muscle cells. A wild-type (left) or a *RECK*$^{-/-}$ (right) embryo stained with anti-SMA. Scale bar: 1 mm in A; 50 μm in B and D; 1 μm in C.

is relatively high in vascular smooth muscle cells (Figure 4B). The result of immunogold electron microscopy also supports this finding (Figure 4C): the flat endothelial cells facing the lumen bear far fewer signals than the cells in the second and third rows. The *RECK* mutation, however, has little impact on the migration and differentiation of smooth muscle cells, as these cells (stained with anti-SMA) are found around the blood vessels in *RECK*$^{-/-}$ embryos (Figure 4D).

Taken altogether, these data suggest that RECK-dependent maintenance of ECM around blood vessels is required for vessel maturation and stabilization, but not for recruitment of the mural cells to the embryonic vasculature.

### Partial Rescue of the RECK Mutant Phenotype by an MMP-2 Null Mutation

To confirm interaction between RECK and MMP-2 (which is extensively expressed at E10; Reponen et al., 1992 and Figure 3K) in vivo, we intercrossed MMP-2 null mice, which, as previously reported (Itoh et al., 1997), exhibited no developmental abnormality (data not shown), with *RECK*$^{+/-}$ mice to generate *MMP-2*$^{-/-}$ *RECK*$^{+/-}$ mice. These mice were found to be healthy and fertile. When we crossed these *MMP-2*$^{-/-}$ *RECK*$^{+/-}$ mice, no *MMP-2*$^{-/-}$ *RECK*$^{-/-}$ double mutants were born. The ratio of the *MMP-2*$^{-/-}$ *RECK*$^{+/+}$ to *MMP-2*$^{-/-}$ *RECK*$^{+/-}$ offspring was about 1:2, indicating a recessive lethal phenotype. At E11.0, about one-third of the *MMP-2*$^{-/-}$ *RECK*$^{-/-}$ animals were still alive, but none of them survived beyond E11.5 (Figure 5A, striped bars). *RECK*$^{-/-}$ embryos were found to die about half a day earlier than the double null mice (Figure 5A, filled bar), indicating that the lethal phenotype in the *RECK*$^{-/-}$ mice was partially rescued by the lack of MMP-2 expression.

It was also noticed that the *MMP-2*$^{-/-}$ *RECK*$^{-/-}$ double mutant embryos were consistently larger in body size than the *RECK*$^{-/-}$ embryos at E10.5 (Figure 5B), and that their tissue integrity was much higher than that of the *RECK*$^{-/-}$ embryos (Figures 5C–5G, compare the middle panels with the right panels). Immunohistochemical analyses indicate that collagen I is detectable in the marginal zone of the neural tubes (Figure 5C) and that the patterns of collagen IV and laminin around the blood vessels and neural tubes are much more organized in the double mutant embryos than the *RECK*$^{-/-}$ embryos (Figures 5D and 5E). Moreover, vascular endothelial cells form tight and thin tubular structures (Figures 5F and 5G), suggesting improved vascular development in the double mutant embryos. These findings suggest that MMP-2 is responsible, at least partially, for the reduced body size, reduced collagen I, and the endothelial disarray found in the E10.5 *RECK*$^{-/-}$ embryos.

### Effects of *RECK* Expression on Tumorigenic Growth of HT1080 Cells

To evaluate the pathophysiological implications of *RECK* expression, HT1080 cells were transfected with either a control vector or a vector expressing *RECK*, and after drug selection, pools of transfectants were inoculated subcutaneously into nude mice. We first compared the size of the tumors at intervals and found no significant difference between the two groups (Figure

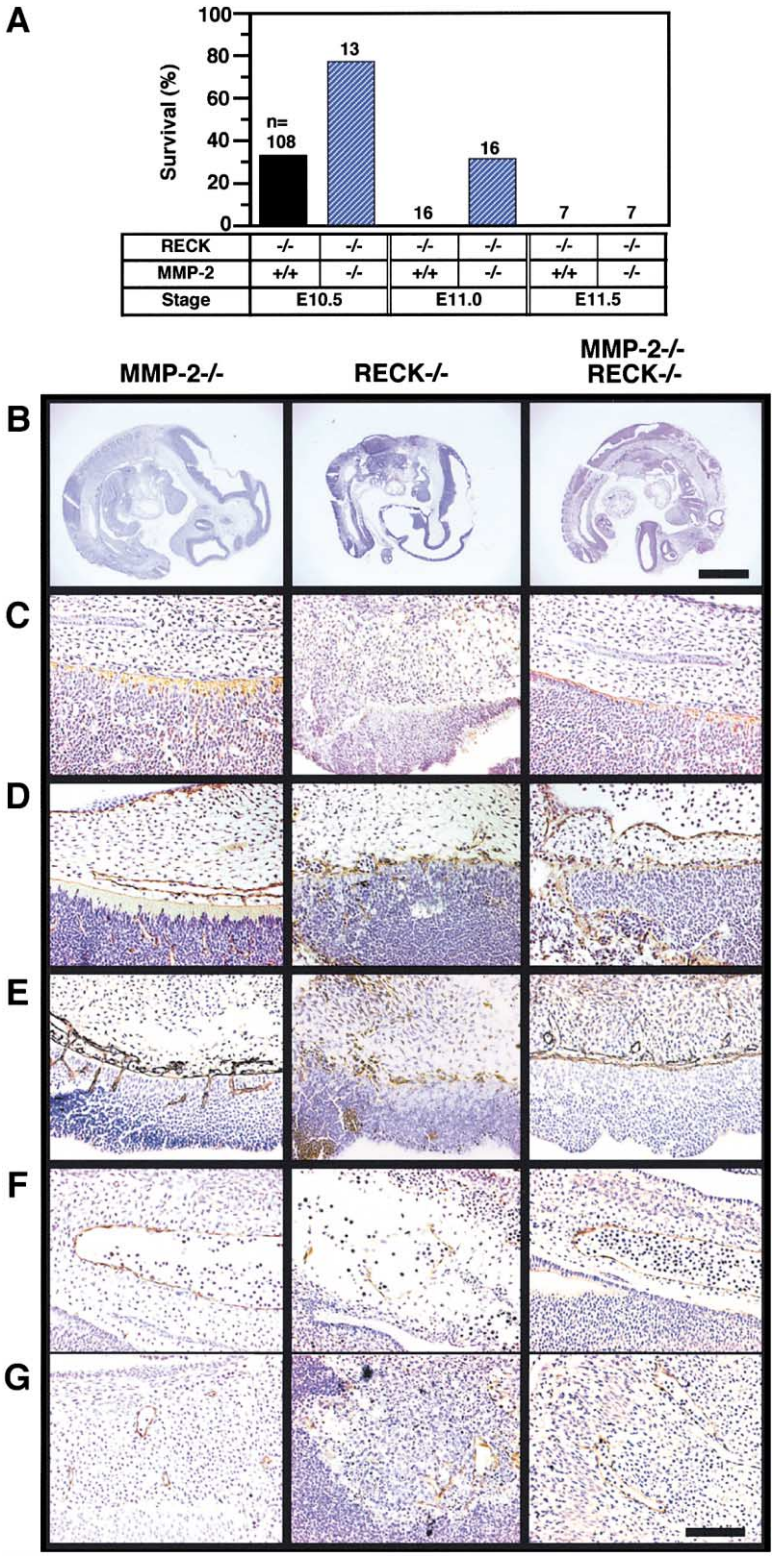


Figure 5. Phenotype of the *MMP-2*$^{-/-}$ *RECK*$^{-/-}$ Double Mutant Mice

(A) Proportion of surviving embryos with indicated genotype at indicated stages. n, number of embryos observed.

(B–G) Sections of the E10.5 embryos with genotypes indicated on the top were stained with hematoxylin-eosin (B) or antibodies against collagen I (C), collagen IV (D), laminin (E), or CD31 (F and G). Scale bar: 1 mm in B; 100 μm in C–G.

6A). It was, however, noted that the animals bearing the *RECK*-expressing tumors tended to live longer than those bearing the control tumors (Figure 6B). Continued expression of RECK in the tumor cells originating from the *RECK* transfectants was confirmed by RNA blot hybridization and immunohistochemical staining (Figures 6C and 6D).

Histological examination of the tumors at different stages revealed that tumor angiogenesis was strongly affected by *RECK* expression. Staining with anti-laminin

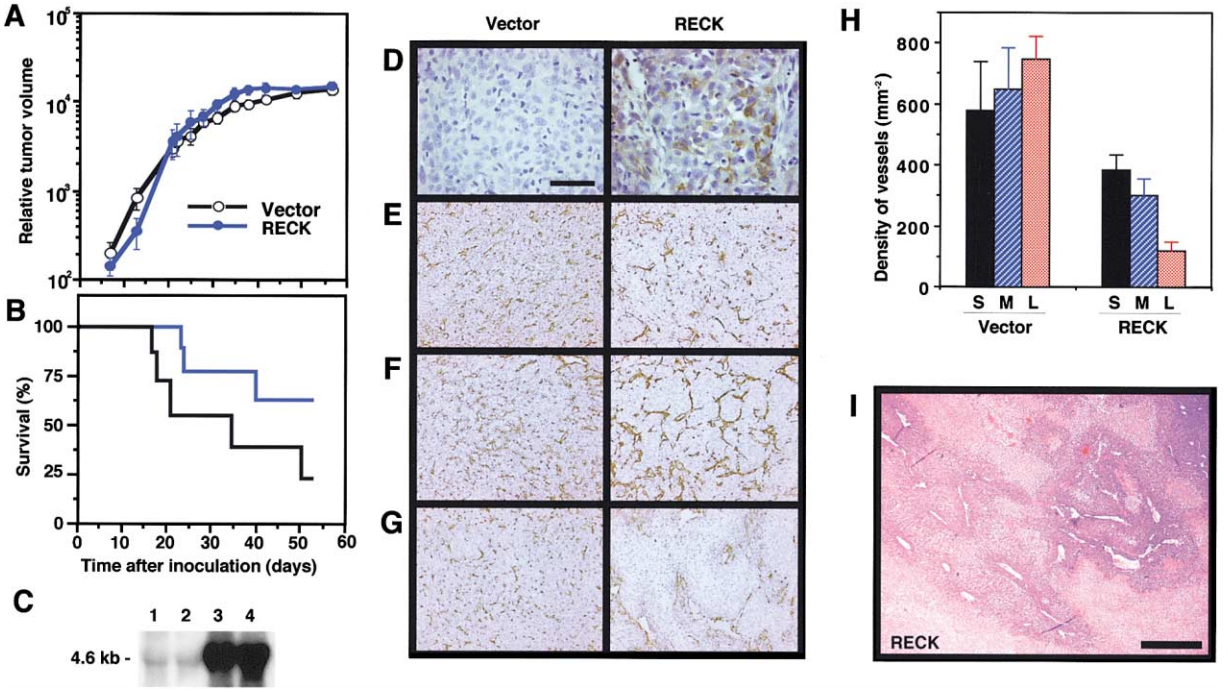


Figure 6. Effects of *RECK* Expression on HT1080-Derived Tumors in Nude Mice

(A) The size of tumors formed after inoculation of HT1080 cells transfected with a control vector (black line) or a vector expressing the *hRECK* gene (blue line). Seven animals were used per group. Note that some animals died during the experiment (see [B]), so the data represent the tumors in surviving animals. The experiments were repeated twice with similar results.

(B) Survival of the animals inoculated with vector-transfected (black line) or *RECK*-transfected (blue line) HT1080 cells. The experiments were repeated twice with similar results. By log-rank test, $P = 0.046$.

(C) Total RNA was extracted from two average-sized tumors arising from vector-transfected cells (lanes 1 and 2) or *RECK*-transfected cells (lanes 3 and 4) on day 11 after inoculation and analyzed by RNA blot hybridization using a *RECK* probe.

(D) Sections were made from the same tumors used in (C) and stained with anti-RECK antibodies.

(E–G) Three animals were sacrificed at three different stages (calculated tumor sizes in $cm^3$: the tumors shown in [E], 0.17 [vector] and 0.21 [RECK]; [F], 0.45 [vector] and 0.67 [RECK]; [G], 6.4 [vector] and 4.6 [RECK]), and the tumors sectioned and then stained with anti-laminin antibodies.

(H) The number of blood vessels in eight randomly picked fields in a section of a small (S, shown in [A]), medium (M, shown in [B]), or large (L, shown in [C]) tumor was counted and are presented as average density per $mm^2$. Vessel density is significantly different only between S and L tumors ($P = 0.02$) arising from vector-transfected cells, but is significantly different between all combinations of tumors arising from RECK-transfected cells ($P < 0.01$).

(I) A hematoxylin-eosin-stained section of a large RECK-expressing tumor whose host survived over 57 days. Scale bar: 50 μm in D; 200 μm in E–G; 500 μm in I.

antibodies, which visualize the basal lamina of blood vessels, clearly demonstrates this effect (Figures 6E–6G). In the control tumors, the density of the blood vessels stayed almost constant as the tumors grew larger (Figures 6E–6G, left panels; Figure 6H, left three bars). In the *RECK*-expressing tumors, however, the density of the blood vessels decreased (Figure 6H). Compartments of cells devoid of blood vessels could be found even in small *RECK*-expressing tumors, and such areas expanded in proportion to the increase in tumor size (Figures 6E–6G, right panels). Figures 6E–6G also illustrate the dramatic increase in vessel cross-sectional area that occurs in RECK-expressing tumors. Essentially the same results were obtained by staining with a marker for endothelial cells (CD31) or for mural cells (α-SMA) (data not shown).

This difference could be explained by assuming that in the *RECK*-expressing tumors, angiogenic sprouting is suppressed, and instead, luminal growth occurred. Consistent with this hypothesis, the majority of the blood vessels in the control tumors show a narrow, thorny morphology characteristic of branching vessels (Figures 6E–6G, left panels), while the proportion of blood vessels with wide-opened lumens (unbranched and/or luminally growing vessels) were significantly higher (2.2–5.5 fold; $P < 0.00023$) in the *RECK*-expressing tumors (Figures 6E–6G and data not shown). Interestingly, in very large *RECK*-expressing tumors, vascularization was limited to a few very large blood vessels, and only the cells surrounding these blood vessels survived, with most cells inside the vessel-free areas dying (Figure 6I). Thus, the expression of RECK at high levels in tumor tissue limits angiogenic sprouting and leads to massive tumor cell death.

## Discussion

Our studies have demonstrated that RECK can inhibit three MMP family members, MMP-2, MMP-9, and MT1-MMP. MMP-2 and MMP-9 efficiently digest denatured

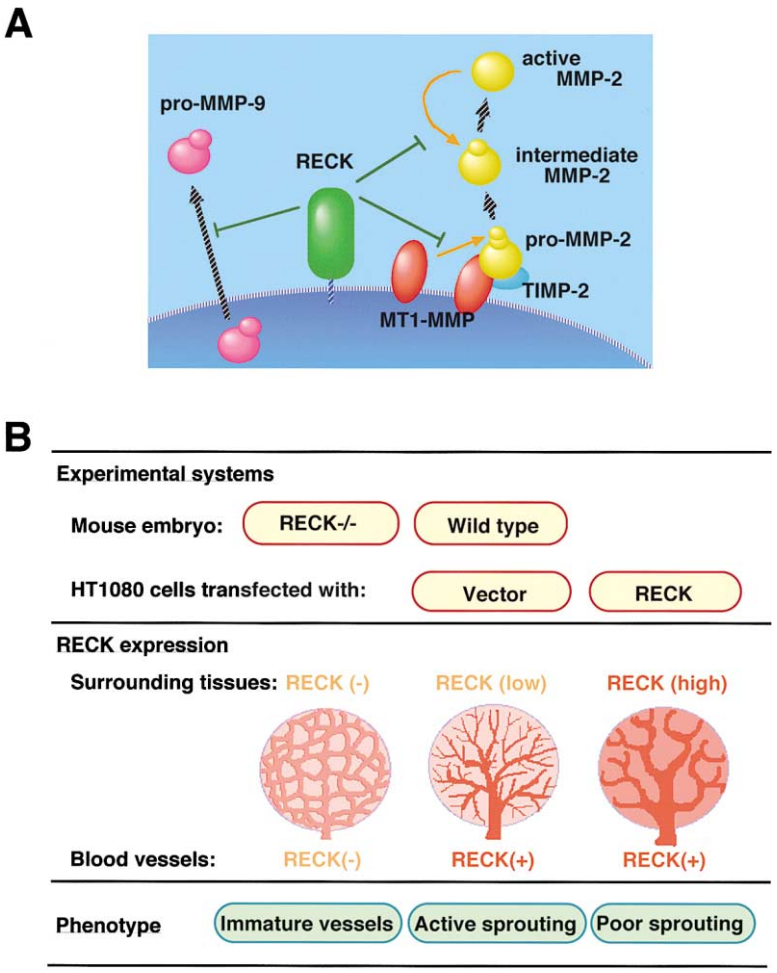


Figure 7. Effects of RECK on MMPs and Angiogenesis

(A) Summary of the effects of RECK on MMPs. RECK is associated with the membrane through GPI-anchoring. RECK apparently inhibits the release of pro-MMP-9 from the cells (Takahashi et al., 1998), and also inhibits the enzyme activity of MT1-MMP and MMP-2, resulting in reduced production of active MMP-2 (this study).

(B) A model to explain our findings in vivo. See text for details.

collagen (Nagase and Woessner, 1999); MT1-MMP not only participates in the processing of pro-MMP-2 but also digests various ECM components in vitro, including collagen I (Pei and Weiss, 1996; Ohuchi et al., 1997). Hence, these MMPs could act alone or in concert to digest collagen fibers, and RECK would inhibit this process. Consistent with this model, collagen fibers around the neural tube, whose peripheral region expresses RECK, MMP-2, and MT1-MMP (Figure 3K), are dramatically reduced in *RECK*-deficient mouse embryos (Figures 3E and 3J). Thus, a simple model to explain the mutant phenotype would be that RECK protects collagen fibrils from degradation catalyzed by these MMPs in the wild-type animal. Our findings that the loss of MMP-2 expression could partially rescue the phenotype of *RECK*$^{-/-}$ mice and that collagen I could be detected in the *MMP-2*$^{-/-}$ *RECK*$^{-/-}$ double mutant embryos at E10.5 suggest that MMP-2 is one of the multiple molecules affected by RECK in vivo and that increased MMP-2 activity is largely responsible for the decreased collagen I seen in the *RECK*$^{-/-}$ mice. Our preliminary results indicate, however, that the loss of MT1-MMP expression fails to rescue the phenotype of *RECK*$^{-/-}$ mice (data not shown). Thus, interaction between MT1-MMP and RECK in vivo remains to be established. Nevertheless, the idea that reduced collagen is causal to the vascular defects is consistent with the earlier finding that mice homozygous for the mutant collagen $\alpha$1(I) gene also die in utero by the rupture of major blood vessels (Lohler et al., 1984).

A group of smaller (20–30 kDa) MMP inhibitors, TIMP-1 to TIMP-4, have been identified and characterized (Brew et al., 2000). A critical difference between RECK and TIMPs lies in their localization: RECK is membrane-anchored, while TIMPs are secreted. Membrane anchoring allows RECK to be concentrated on the plasma membrane (unpublished data) and to effectively regulate local proteolytic events at the cell surface, where proteolytic processing of MMPs occurs (Werb, 1997). Additionally, the lack of RECK is embryonic lethal in mice, while the lack of TIMP-1 or TIMP-2 has little effect on development (Nothnick et al., 1997; Wang et al., 2000; Caterina et al., 2000), suggesting that RECK shares little functional redundancy with the TIMPs, at least during this stage (E10.5) of mouse development.

Ras is known to affect cell-ECM interaction in several ways: activated Ras downregulates several ECM proteins, such as fibronectin and collagen I, as well as ECM-receptors (integrins) (Fagan et al., 1981; Howard et al., 1978; Plantefaber and Hynes, 1989), while it upregulates several MMPs (Garbisa et al., 1987; Thant et al., 1997). These changes contribute in concert to the manifestation of the transformed phenotype, especially reduced adhesion to the substrate. Our findings add another

essential component to this picture: RAS-mediated downregulation of RECK, which allows the MMPs to elicit their full activity.

Figure 7 illustrates an interpretation of our findings in vivo. In the *RECK*$^{-/-}$ E10.5 mouse embryos, RECK is not expressed in blood vessels or in the surrounding tissue; under these conditions, vasculogenesis occurs, but maturation of the vasculature is compromised (Figure 7B, left cartoon). In the wild-type embryo, RECK is expressed in blood vessel cells, especially in mural cells, while its expression is low in the surrounding tissue. The situation is likely to be similar in the control HT1080 tumors proliferating in nude mice: due to the activated N-*ras* oncogene expressed by HT1080 cells (Brown et al., 1984), RECK is downregulated in the tumor tissue (see Figure 1), while the blood vessel cells are of mouse origin and probably express RECK. Under these conditions, the integrity of the blood vessels is not impaired, nor is angiogenic sprouting inhibited (Figure 7B, middle cartoon). In the RECK-expressing HT1080 tumors, however, the vasculature is defective. In these tumors, the defect is not due to the inability of the vasculature to mature, but rather to inhibition of angiogenic sprouting (Figure 7B, right cartoon). A simple model can explain these findings: in the absence of RECK expression, excess MMP activity results in excessive degradation of the ECM, causing reduced structural integrity of the blood vessels (and perhaps of the surrounding tissue). This in turn retards maturation of the early vascular network. In the presence of high RECK expression, MMP activity is reduced to the point where ECM remodeling is compromised and the ability of preexisting blood vessels to send out capillary sprouts and produce new vessels is inhibited. Thus, the magnitude and spatial pattern of RECK and MMP activity are crucial for normal angiogenesis: high RECK and low MMP activity would be predominant in areas where angiogenesis is suppressed, e.g., around the major arteries, and lower RECK and higher MMP activity would be predominant in areas where angiogenesis normally occurs.

However, it is unclear exactly why vascular development stops when RECK is absent. While our biochemical and histological data suggest that accelerated degradation of ECM components, such as collagen I, is likely to be the primary consequence of RECK-deficiency, it is possible that RECK also regulates the amount or fate of certain extracellular signaling molecules (e.g. transforming growth factor-β, vascular endothelial growth factor, thrombospondin, etc.), which in turn regulate collagen production or other aspects of angiogenesis (Vu and Werb, 2000). Further studies using the experimental systems described here may help in identifying an additional molecular target(s) for RECK in vivo.

Good correlation has been found between the abundance of *RECK* expression in hepatoma samples and the survival of the patients (Furumoto et al., 2001). This finding is reminiscent of the survival curve of nude mice bearing RECK-expressing HT1080 tumors (Figure 6B). Thus, *RECK* expression can be a good prognostic indicator for cancer patients. Moreover, since overexpression of *RECK* in tumors was found to affect tumor angiogenesis as well as invasion and metastasis, application of the *RECK* gene, the RECK protein, its chemical mimetic, or drugs activating endogenous *RECK* expression should be evaluated as possible therapeutic or preventive agents for cancer.

## Experimental Procedures

### Cell Culture

HT1080 (human fibrosarcoma) cells were maintained in growth medium (GM) as described previously (Kitayama et al., 1989). The cells ($3 \times 10^4$/35 mm dish) were transfected with the mammalian expression vector pCXN2 (Niwa et al., 1991) or pCXN2 containing human *RECK* (*hRECK*) cDNA (2 μg) by the standard calcium phosphate method, and after selection for 10 days with GM containing 1 mg/ml G418, stable transfectant colonies were pooled and passaged several times (1:20, every 3–4 days) in the selection medium before being used for experiments. Methods for preparing conditioned media and gelatin zymography have been described elsewhere (Takahashi et al., 1998).

### Determination of MMP Activity

The same fluorescent peptide, (7-methoxycoumarin-4-yl)Acetyl-Pro-Leu-Gly-Leu-(3-[2,4-dinitrophenyl]-L-2,3-diaminopropionly)-Ala-Arg-$NH_2$ (Mca-P-L-G-L-Dpa-A-R) (Peptide Institute, Osaka, Japan) (Knight et al., 1992), was used as the substrate in the following three types of assays:

***(1) MT1-MMP***

An aliquot of MT1-F protein (soluble FLAG-tagged MT1-MMP) expressed in *E. coli* and immobilized on anti-FLAG M2 beads (IHI) as described previously (Kinoshita et al., 1998) was incubated in 50 μl assay buffer (0.1 M Tris-HCl [pH 7.5], 0.1 M NaCl, 10 mM $CaCl_2$, and 0.05% Brij-35) containing 10 μM substrate with or without BSA (4 pmol), hRECKΔC (2 or 4 pmol), or TIMP-2 (0.25 pmol) at 25°C for 20 min. The reaction was terminated by adding 80 μl of 0.1 M sodium acetate (pH 4.0), and the hydrolysis of the substrate was measured with a spectrofluorimeter (Shimazu RF-1500; λex = 328 nm, λem = 393 nm) at 25°C.

***(2) MMP-2***

Pro-MMP-2 (1 μg, Boehringer Mannheim) was activated in 5 μl of 0.75 mM APMA, 20 mM Tris-HCl (pH 7.5), 50 mM NaCl, and 10 mM $CaCl_2$ at 37°C for 5 min. At this time point, about 80% of the maximum level of activation was achieved, and further incubation gave rise to smaller degradation products (data not shown). Immediately after activation, the enzyme (0.25 μg) was mixed with different amounts of substrate in the presence or absence of hRECKΔC (3.5 pmol) in 50 μl assay buffer and incubated at 25°C for 10 min. The $K_i$ value was calculated using the equation $1/V = 1/V_{max} + K_m\,(1 + [I]/K_i)/V_{max}\,[S]$.

***(3) Conditioned Media***

MMP activity in an aliquot (the amount corresponding to $3 \times 10^4$ cells) of conditioned medium was measured in a 50 μl reaction mixture as described in (1) without addition of any other proteins.

### RNA Blot Hybridization and Immunoblot Assay

Total RNA was extracted and analyzed by RNA blot hybridization using $^{32}$P-labeled mouse or human *RECK* cDNA (Takahashi et al., 1998), human MT1-MMP cDNA (Sato et al., 1994), human TIMP-2 cDNA, or human glyceraldehyde-3-phosphate dehydrogenase (GAPDH) cDNA. To extract proteins, cultured cells or mouse embryos were homogenized in 50 mM Tris.HCl (pH 6.8), 1% SDS, 1 mM EDTA containing 1 mM PMSF, 16 mM soybean trypsin inhibitor, and 3.5 mM aprotinin. The lysates were cleared by centrifugation, and their protein concentration determined. The sample (70 μg protein) was separated by SDS-PAGE (10% acrylamide), followed by immunoblot detection using monoclonal antibodies against RECK (5B11D12), MT1-MMP (114-6G6), or MMP-2 (42-5D11). For visualization, the Enhanced Chemiluminescence kit (Amersham) was used with HRP-conjugated anti-mouse IgG-F(ab′)2 monoclonal antibody (Wako).

### Generation of Mutant Mice

Fragments of the mouse *RECK* gene were cloned from the λFixII-129/Sv genomic library (Stratagene) (Sasahara et al., 1999). The 4.0 kilobase (kb) SpeI-SmaI fragment upstream of the first exon and the 2.5 kb HindIII fragment downstream of the first exon were in-

serted into the XbaI and HindIII sites, respectively, of the PGK-neo-DTA vector (Yagi et al., 1990). This targeting vector was linearized with NotI and introduced by electroporation into E14 ES cells. G418-resistant clones carrying the mutant allele were selected and injected into C57BL/6J blastocysts (Gomi et al., 1995). Chimeric males, identified by coat color, were bred to C57BL/6J and 129/Sv females.

Generation, genotyping, and characterization of MMP-2-deficient mice have been described (Itoh et al., 1997). The *RECK*$^{+/-}$ mice were first backcrossed into the C57BL/6 strain five generation and then intercrossed with the *MMP-2*$^{-/-}$ mice to generate *MMP-2*$^{+/-}$ *RECK*$^{+/-}$ mice. These double heterozygotes were crossed to obtain *MMP-2*$^{-/-}$ *RECK*$^{+/-}$ mice which were then crossed each other to obtain *MMP2*$^{-/-}$ *RECK*$^{-/-}$ embryos.

### Genotype Analyses for RECK Mutant Mice

Targeted mutation of the *RECK* locus in ES clones was confirmed by Southern blot assay using BamHI and the 5′-flanking probe (Figure 2A), which discriminates between wild-type (28 kb) and mutant (23 kb) alleles. Transmission of the mutant allele in mice was routinely detected by PCR using yolk sac or tail DNA with the following primer sets and was confirmed, when necessary, by Southern blot assay. Primer set (1) yielding a 350 base pair (bp) wild-type band: forward 5′-TTGGCTTTGAGGGGAGGCCAGGTAACACGC-3′; reverse 5′-CCCTGGACCCTGGCTCTTTGTTATGGGCCA-3′. Primer set (2) yielding a 270 bp mutant-specific *neo*-derived band: forward 5′-CTTGGGTGGAGAGGCTATTC-3′; reverse 5′-AGGTGAGATGA CAGGAGATC-3′.

### Immunohistochemical Analyses

Sections (5 μm thick) of formalin-fixed, paraffin-embedded embryos or tumors were prepared and stained as described elsewhere (Matsuo et al., 1999) using chromogen 3, 3-diaminobenzidine-HCl (stains brown) followed by nuclear counterstaining with hematoxilin (stains purple). The primary antibodies used were: RECK (5B11D12; Takahashi et al., 1998); CD31 (PharMingen, #01951); α-smooth muscle actin (1A4, Dako, M0851); collagen I (Rockland, #600-401-103); collagen IV (Takara, M119); laminin (Progen, #10765); MMP-2 (42-5D11, Fuji, F68); MT1-MMP (Chemicon, AB815). Whole-mount immunostaining with the anti-CD31 or anti-Flk-1 antibodies (AVAS12β) was performed as described by Schlaeger et al. (1995).

### In Situ Zymography

Mouse embryos were embedded in Tissue-Tek OCT compound (Miles, Elkhart, IN), immediately frozen, sliced (6 μm thick) using cryostat, and processed as described by Ikeda et al. (2000). The film was stained with 1.0% Amido Black 10B.

### Electron Microscopy

Embryos were cut horizontally at the abdominal level and immersed in Zamboni's fixative for 4–6 hr. Samples were then rinsed in 0.1 M phosphate buffer (pH 7.4), post-fixed with 1% osmium tetroxide, immersed in 0.5% uranyl acetate overnight, dehydrated with a graded series of aquaous ethanol, and embedded in epoxy resin. Ultrathin sections were cut, stained with 5% uranyl acetate and Raynolds' lead citrate, and examined with a transmission electron microscope, Hitachi H-8100. Immunoelectron microscopy was performed as described previously (Kinoshita et al., 1997) using anti-RECK antibodies (5B11D12; 1:250).

### Culture and Analyses of Embryonic Cells

E10.5 embryos were broken into 20–30 pieces by mild pipetting in 2 ml PBS. The tissue pieces were collected by brief centrifugation, resuspended in 0.5 ml αMEM containing 40% fetal calf serum plus antibiotics, and plated onto a collagen-coated 35 mm dish. After overnight incubation, the cells were fed with 1.5 ml medium and the incubation was continued for several days until the culture reached confluence. The cells were trypsinized, dispersed by mild pipetting (allowing preservation of residual cell clumps), plated at a 1:3 splitting ratio, and incubated for 3–4 days. After 4 cycles of such passaging, the cells were thoroughly dispersed by trypsinization and seeded onto a collagen-coated 12 well plate ($5 \times 10^5$ per well). After 24 hr incubation, conditioned medium was prepared and analyzed by gelatin zymography. MEF were established by continued passaging (more than 35 times) of these cultures.

### Formation and Analyses of Tumors in Nude Mice

HT1080 cells transfected with empty pCXN2 or pCXN2 containing *hRECK* cDNA were trypsinized, suspended at $5 \times 10^7$/ml in PBS containing antibiotics, and inoculated subcutaneously into the back of 4 week old female Balb/c nu/nu mice (0.2 ml per site/animal; n = 10). Sizes (length, width, and height) of the tumors were measured weekly, and three animals were sacrificed at appropriate time points for histological examination. Survival of the remaining 7 animals was monitored 2–3 times a week. The experiments using mice were carried out following institutional guidelines. Measurements on microscopic images were carried out using the software NIH Image.

### Acknowledgments

We thank M. Hooper for the E14 ES cells, Thomas N. Sato for the protocol for whole-mount immunostaining, Masatoshi Maki for technical advice, Ryoichi Nemori (FUJIFILM) for the FIZ materials, Emi Nishimoto and Takashi Kawai for technical assistance, and Aki Miyazaki for secretarial assistance. We are also grateful to Drs. Yoji Ikawa and Haruo Sugano for generous support and encouragement and to Drs. Robert A. Weinberg and Rudolf Jaenisch for discussion. This work was supported by grants from the Ministry of Education, Science, Sports, and Culture of Japan to C.T. and M.N. and from Amgen, Sankyo, Co. Ltd., and Takeda Science Foundation to M.N.

Received May 14, 2001; revised October 23, 2001.

### References

Birkedal-Hansen, H. (1995). Proteolytic remodeling of extracellular matrix. Curr. Opin. Cell Biol. *7*, 728–735.

Brew, K., Dinakarpandian, D., and Nagase, H. (2000). Tissue inhibitors of metalloproteinases, evolution, structure and function. Biochim. Biophys. Acta *1477*, 267–283.

Brown, R., Marshall, C.J., Pennie, S.G., and Hall, A. (1984). Mechanism of activation of an N-ras gene in the human fibrosarcoma cell line HT1080. EMBO J. *3*, 1321–1326.

Canete-Soler, R., Gui, Y., Linask, K.K., and Muschel, R.J. (1995). Developmental expression of MMP-9 (Gelatinase B) mRNA in mouse embryos. Dev. Dyn. *204*, 30–40.

Caterina, J.J., Yamada, S., Caterina, N.C.M., Longenecker, G., Holmback, K., Shi, J., Yermovsky, A.E., Engler, J.A., and Birkedal-Hansen, H. (2000). Inactivating mutation of the mouse tissue inhibitor of metalloproteinase-2 (Timp-2) gene alters proMMP-2 activation. J. Biol. Chem. *275*, 26416–26422.

Coussens, L.M., Tinkle, C.L., Hanahan, D., and Werb, Z. (2000). MMP-9 supplied by bone marrow-derived cells contribute to skin carcinogenesis. Cell *103*, 481–490.

Davies, B., Waxman, J., Wasan, H., Abel, P., Williams, G., Krausz, T., Neal, D., Thomas, D., Hanby, A., and Balkwill, F. (1993). Levels of matrix metalloproteases in bladder cancer correlate with tumor grade and invasion. Cancer Res. *53*, 5365–5369.

Ellerbroek, S.M., and Stack, M.S. (1999). Membrane associated matrix metalloproteinases in metastasis. Bioessays *21*, 940–949.

Fagan, J.B., Sobel, M.E., Yamada, K.M., de Crombrugghe, B., and Pastan, I. (1981). Effects of transformation on fibronectin gene expression using cloned fibronectin cDNA. J. Biol. Chem. *256*, 520–525.

Folkman, J., and D'Amore, P.A. (1996). Blood vessel formation: what is its molecular basis? Cell *87*, 1153–1155.

Furumoto, K., Arii, S., Mori, A., Furuyama, H., Gorrin Rivas, M.J., Nakao, T., Isobe, N., Murata, T., Takahashi, C., Noda, M., and Imamura, M. (2001). RECK gene expression in hepatocellular carcinoma, Correlation with invasion-related clinicopathological factors and its clinical significance. Hepatology *33*, 189–195.

Garbisa, S., Pozzatti, R., Muschel, R.J., Saffiotti, U., Ballin, M., Goldfarb, R.H., Khoury, G., and Liotta, L.A. (1987). Secretion of type IV collagenolytic protease and metastatic phenotype, induction by

transfection with c-Ha-ras but not c-Ha-ras plus Ad2–E1a. Cancer Res. *47*, 1523–1528.

Gomi, H., Yokoyama, T., Fujimoto, K., Ikeda, T., Katoh, A., Itoh, T., and Itohara, S. (1995). Mice devoid of the glial fibrillary acidic protein develop normally and are susceptible to scrapie prions. Neuron *14*, 29–41.

Hanahan, D. (1997). Signaling vascular morphogenesis and maintenance. Science *277*, 48–50.

Hanahan, D., and Folkman, J. (1996). Patterns and emerging mechanisms of the angiogenic switch during tumorigenesis. Cell *86*, 353–364.

Hidalgo, M., and Eckhardt, S.G. (2001). Development of matrix metalloproteinase inhibitors in cancer therapy. J. Natl. Cancer Inst. *93*, 178–193.

Howard, B.H., Adams, S.L., Sobel, M.E., Pastan, I., and de Crombrugghe, B. (1978). Decreased levels of collagen mRNA in rous sarcoma virus-transformed chick embryo fibroblasts. J. Biol. Chem. *253*, 5869–5874.

Ikeda, M., Maekawa, R., Tanaka, H., Matsumoto, M., Takeda, Y., Tamura, Y., Nemori, R., and Yoshioka, T. (2000). Inhibition of gelatinolytic activity in tumor tissues by synthetic matrix metalloproteinase inhibitor: application of film in situ zymography. Clin. Cancer Res. *6*, 3290–3296.

Itoh, T., Ikeda, T., Gomi, H., Nakao, S., Suzuki, T., and Itohara, S. (1997). Unaltered secretion of β-amyloid precursor protein in gelatinase A (Matrix Metalloproteinase 2)-deficient mice. J. Biol. Chem. *272*, 22389–22392.

Kahari, V.M., and Saarialho-Kere, U. (1999). Matrix metalloproteinases and their inhibition in tumour growth and invasion. Ann. Med. *31*, 34–45.

Kitayama, H., Sugimoto, Y., Matsuzaki, T., Ikawa, Y., and Noda, M. (1989). A ras-related gene with transformation suppressor activity. Cell *56*, 77–84.

Kinoshita, M., Kumar, S., Mizoguchi, A., Ide, C., Kinoshita, A., Haraguchi, T., Hiraoka, Y., and Noda, M. (1997). Nedd5, a mammalian septin, is a novel cytoskeletal component interacting with actin-based structures. Genes Dev. *11*, 1535–1547.

Kinoshita, T., Sato, H., Okada, A., Ohuchi, E., Imai, K., Okada, Y., and Seiki, M. (1998). TIMP-2 promotes activation of progelatinase A by membrane-type 1 matrix metalloproteinase immobilized on agarose beads. J. Biol. Chem. *273*, 16098–16103.

Knight, C.G., Willenbrock, F., and Murphy, G. (1992). A novel coumarin-labelled peptide for sensitive continuous assays of the matrix metalloproteinases. FEBS Lett. *296*, 263–266.

Lohler, J., Timpl, R., and Jaenisch, R. (1984). Embryonic lethal mutation in mouse collagen I gene causes rupture of blood vessels and is associated with erythropoietic and mesechymal cell death. Cell *38*, 597–607.

Matsuo, S., Sugiyama, T., Okuyama, T., Yoshikawa, K., Honda, K., Takahashi, R., and Maeda, S. (1999). Preservation of pathological tissue specimens by freeze-drying for immunohisochemical staining and various molecular biological analyses. Pathol. Int. *49*, 383–390.

Nagase, H., and Woessner, J.F., Jr. (1999). Matrix metalloproteinases. J. Biol. Chem. *274*, 21491–21494.

Niwa, H., Yamamura, K., and Miyazaki, J. (1991). Efficient selection for high-expression transfectants with a novel eukaryotic vector. Gene *108*, 193–199.

Noda, M., Kitayama, H., Matsuzaki, T., Sugimoto, Y., Okayama, H., Bassin, R.H., and Ikawa, Y. (1989). Detection of genes with a potential for suppressing the transformed phenotype associated with activated ras genes. Proc. Natl. Acad. Sci. USA *86*, 162–166.

Nothnick, W.B., Soloway, P., and Curry, T.E., Jr. (1997). Assessment of the role of tissue inhibitor of metalloproteinase-1 (TIMP-1) during the periovulatory period in female mice lacking a functional TIMP-1 gene. Biol. Reprod. *56*, 1181–1188.

Ohuchi, E., Imai, K., Fujii, Y., Sato, H., Seiki, M., and Okada, Y. (1997). Membrane type 1 matrix metalloproteinase digests interstitial collagens and other extracellular matrix macromolecules. J. Biol. Chem. *272*, 2446–2451.

Pei, D., and Weiss, S.J. (1996). Transmembrane-deletion mutants of the membrane-type matrix metalloproteinase-1 process progelatinase A and express intrinsic matrix-degrading activity. J. Biol. Chem. *271*, 9135–9140.

Plantefaber, L.C., and Hynes, R.O. (1989). Changes in integrin receptors on oncogenically transformed cells. Cell *56*, 281–290.

Reponen, P., Sahlberg, C., Huhtala, P., Hurskainen, T., Thesleff, I., and Tryggvason, K. (1992). Molecular cloning of murine 72-kDa type IV collagenase and its expression duirng mouse development. J. Biol. Chem. *267*, 7856–7862.

Risau, W. (1997). Mechanisms of angiogenesis. Nature *386*, 671–674.

Sasahara, R.M., Takahashi, C., and Noda, M. (1999). Involvement of the Sp1 site in ras-mediated downregulation of the RECK metastasis suppressor gene. Biochem. Biophys. Res. Commun. *264*, 668–675.

Sato, H., Takino, T., Okada, Y., Cao, J., Shinagawa, A., Yamamoto, E., and Seiki, M. (1994). A matrix metalloproteinase expressed on the surface of invasive tumor cells. Nature *370*, 61–65.

Schlaeger, T.M., Qin, Y., Fujiwara, Y., Magram, J., and Sato, T.N. (1995). Vascular endothelial cell lineage-specific promoter in transgenic mice. Development *121*, 1089–1098.

Stetler-Stevenson, W.G. (1999). Matrix metalloproteinasese in angiogenesis: a moving target for therapeutic intervention. J. Clin. Inv. *103*, 1237–1241.

Takahashi, C., Akiyama, N., Matsuzaki, T., Takai, S., Kitayama, H., and Noda, M. (1996). Characterization of a human MSX-2 cDNA and its fragment isolated as a transformation suppressor gene against v-Ki-ras oncogene. Oncogene *12*, 2137–2146.

Takahashi, C., Sheng, Z., Horan, T.P., Kitayama, H., Maki, M., Hitomi, K., Kitaura, Y., Takai, S., Sasahara, R.M., Horimoto, A., et al. (1998). Regulation of matrix metalloproteinase-9 and inhibition of tumor invasion by the membrane-anchored glycoprotein RECK. Proc. Natl. Acad. Sci. USA *95*, 13221–13226.

Thant, A.A., Serbulea, M., Kikkawa, F., Liu, E., Tomoda, Y., and Hamaguchi, M. (1997). c-Ras is required for the activation of the matrix metalloproteinases by concanavalin A in 3Y1 cells. FEBS Lett. *406*, 28–30.

Vu, T.H., and Werb, Z. (2000). Matrix metalloproteinases, effectors of development and normal physiology. Genes Dev. *14*, 2123–2133.

Wang, Z., Juttermann, R., and Soloway, P.D. (2000). TIMP-2 is required for efficient activation of proMMP-2 in vivo. J. Biol. Chem. *275*, 26411–26415.

Werb, Z. (1997). ECM and cell surface proteolysis, regulating cellular ecology. Cell *91*, 439–442.

Yagi, T., Ikawa, Y., Yoshida, K., Shigetani, Y., Takeda, N., Mabuchi, I., Yamamoto, T., and Aizawa, S. (1990). Homologous recombination at c-fyn locus of mouse embryonic stem cells with use of diphtheria toxin A-fragment gene in negative selection. Proc. Natl. Acad. Sci. USA *87*, 9918–9922.

Yamamoto, M., Mohanam, S., Sawaya, R., Fuller, G., Seiki, M., Sato, H., Gokaslan, Z.L., Liotta, L.A., Nicolson, G.L., and Rao, J.S. (1996). Differential expression of membrane-type matrix metalloproteinase and its correlation with gelatinase A activation in human malignant brain tumors in vivo and in vitro. Cancer Res. *56*, 384–392.

Yancopoulos, G.D., Davis, S., Gale, N.W., Rudge, J.S., Wiegand, S.J., and Holash, J. (2000). Vascular-specific growth factors and blood vessel formation. Nature *407*, 242–248.